Dielectric map of the Martian northern hemisphere and the nature of plain filling materials

Jérémie Mouginot, Antoine Pommerol, Pierre Beck, Wlodek Kofman, Stephen M. Clifford

Dielectric map of the Martian northern hemisphere and the nature of plain filling materials

Jérémie Mouginot,[1,2] Antoine Pommerol,[1,3] Pierre Beck,[1] Wlodek Kofman,[1] and Stephen M. Clifford[4]

Received 9 November 2011; revised 13 December 2011; accepted 13 December 2011; published 19 January 2012.

[1] A number of observations suggest that an extended ocean once covered a significant part of the Martian northern hemisphere. By probing the physical properties of the subsurface to unprecedented depth, the MARSIS/Mars Express provides new geophysical evidences for the former existence of a Late Hesperian ocean. The Vastitas Borealis formation, located inside a putative shoreline of the ancient ocean, has a low dielectric constant compared with that of typical volcanic materials. We show that the measured value is only consistent with low-density sedimentary deposits, massive deposits of ground-ice, or a combination of the two. In contrast, radar observations indicate a distribution of shallow ground ice in equilibrium with the atmosphere in the south polar region. We conclude that the northern plains are filled with remnants of a late Hesperian ocean, fed by water and sediments from the outflow channels about 3 Gy ago.
Citation: Mouginot, J., A. Pommerol, P. Beck, W. Kofman, and S. M. Clifford (2012), Dielectric map of the Martian northern hemisphere and the nature of plain filling materials, *Geophys. Res. Lett.*, *39*, L02202, doi:10.1029/2011GL050286.

1. Introduction

[2] The surface geology of Mars attests that water was once flowing in abundance. The action of liquid water deeply eroded the Martian upper crust, creating dendritic valleys networks [*Carr*, 1996; *Luo and Stepinski*, 2009; *Di Achille and Hynek*, 2010] and wide outflow channels through which massive amounts of sediments were transported and redistributed [*Carr*, 1987; *Baker et al.*, 1991]. This erosion occurred episodically from the Late Noachian through the Early Amazonian, about 4–2 billion years ago.

[3] Based on the identification of possible paleoshorelines surrounding the northern plains of Mars, it has been argued that the planet may have once hosted "Oceanus Borealis", a hemispheric ocean that covered more than 30% of the planet's surface [*Baker et al.*, 1991; *Parker et al.*, 1993; *Clifford and Parker*, 2001]. Topographic data has been cited to both support [*Head et al.*, 1999; *Clifford and Parker*, 2001] and question [*Carr and Head*, 2003] the consistency of these plains margins with equipotential surfaces, potentially indicative of past sea levels. More recently, it has been demonstrated [*Perron et al.*, 2007] that the elevations of these proposed shorelines closely conform to past equipotential surfaces that were later deformed by crustal movement associated with true polar wander. Additional support for the presence of a Noachian-age ocean comes from a recent study of the distribution of the Martian valley networks and the observation of iso-altitude deltaic deposits [*Luo and Stepinski*, 2009; *Di Achille and Hynek*, 2010].

[4] However, several workers [*Malin and Edgett*, 1999; *Tanaka et al.*, 2001; *Carr and Head*, 2003] have questioned the true nature of the contacts interpreted as paleoshorelines [*Parker et al.*, 1989; *Parker et al.*, 1993] as their characteristics, revealed by MOC high resolution images, might also be explained by a volcanic origin. In addition, long and high ridges across the plains are interpreted as indications of the volcanic filling of lowlands during the early Hesperian [*Head et al.*, 2002]. The total thickness of the volcanic materials could exceed a kilometer and totally hide the remnants of the hypothetical Noachian ocean. Thus, the absence of evaporites and the relatively low abundance of altered minerals found across the northern plains by orbital spectrometers may not place a strong constraint on the former presence of a Noachian ocean.

[5] If any remnant of a Noachian ocean still survives, it should be deeply buried. However, potential evidence of the last stage of the ocean's evolution is visible on the surface. The peak in outflow channel activity occurred around the Hesperian-Amazonian transition, which postdates the principal era of volcanic activity over much of the northern plains. These events transported and deposited significant amounts of water and sediment, which covered the northern lowlands. Indeed, the Vastitas Borealis Formation (VBF), has been identified [*Kreslavsky and Head*, 2002] as a thin (~100 m-thick) sedimentary veneer that overlies the volcanic ridged plains. As such, it represents the best geologic evidence to date for the existence of a Late Hesperian ocean.

2. Data and Methodology

[6] The MARSIS/Mars Express low-frequency sounding radar was designed to probe the Martian subsurface to depths of up to four kilometres in the ice-rich polar layered deposits (PLD) and to depths of up to several hundred meters in the lithic environments that characterized everywhere else, providing new insights into the nature of the crust [*Picardi et al.*, 2005; *Mouginot et al.*, 2010]. These data strongly contrast with other remote-sensing methods that can only probe the surface to depths of ~1 μm to 1 mm in the visible and infrared; ~0.5 m for neutrons, gamma- and X-rays; and in-situ analyses by landers and rovers that can

[1]Institut de Planétologie et d'Astrophysique de Grenoble, CNRS/UJF, France.
[2]Department of Earth System Science, University of California, Irvine, California, USA.
[3]Space Research and Planetary Sciences Division, Physikalisches Institut, Universität Bern, Bern, Switzerland.
[4]Lunar and Planetary Institute, Houston, Texas, USA.

0094-8276/12/2011GL050286

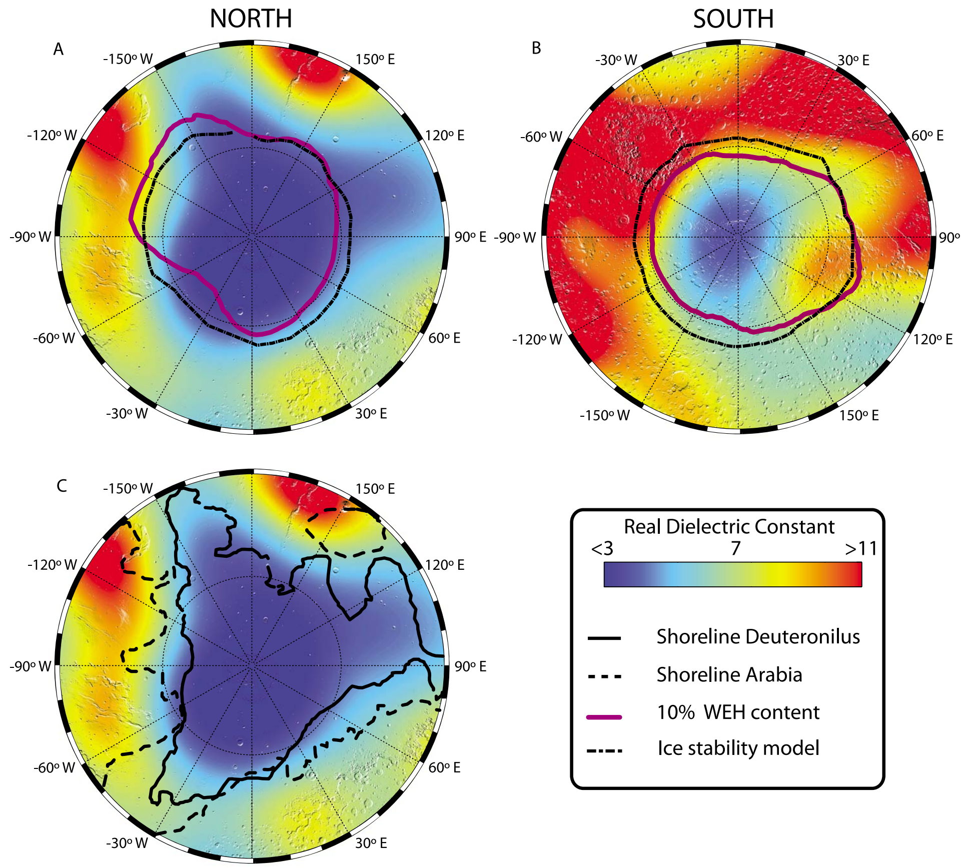

Figure 1. Maps of the Martian (a, c) northern and (b) southern hemisphere, from 30°S to the pole, displayed in polar stereographic projection. The blue-red colors represent the surface dielectric values measured by MARSIS and interpolated by spherical harmonics of order 8. Base map is a Mars Orbiter Laser Altimeter (MOLA) shaded-relief image. Low values (blue) are best explained by low density materials and/or presence of ice, while high values (red) indicate the presence of higher density volcanic materials. The contour-line of 10% Water Equivalent Hydrogen (WEH) in the shallow subsurface [*Feldman et al.*, 2002] and the current theoretical stability limit of ground ice [*Schorghofer and Aharonson*, 2005] are overlaid onto the MARSIS map. Comparison between these datasets (neutrons, recent polygons, and MARSIS) shows that, in the south, the current distribution of shallow subsurface ice is generally consistent with the theoretical stability limit of ground ice in equilibrium with the current surface temperature and water vapour content of the atmosphere (Figure 1b). Contrary to the southern hemisphere, the region with low dielectric value mapped by MARSIS extends equatorward far beyond the latitudes where shallow subsurface ice is expected to be stable (Figure 1a).

reach depths of ∼5–20 cm, e.g., Phoenix detected ice at a depth of 5 cm [*Mellon et al.*, 2009].

[7] *Mouginot et al.* [2010] derived a 3–5 MHz global dielectric map based on the extraction of the surface reflectivity from two years of MARSIS measurements that provides insights into the average composition and physical properties of the first 60 to 80 meters below the surface. Additional data acquired since this time have been included to produce the updated dielectric maps shown in Figure 1 with greater spatial coverage of the northern hemisphere. The ability of sounding radar to probe deep into the crust provides insights into events and conditions that occurred further back in time – which, in the context of the VBF, is though to date back ∼2–3 billion years. Radar probes the nature of planetary subsurfaces by revealing contrasts of dielectric constant ε. In the case of Mars, ε is influenced by two main parameters: the density of the materials and the amount of ice in the ground. Dense volcanic materials can have dielectric constants as high as 10 at 2 MHz. Decreasing the density of the materials results in a decrease of ε. Since pure water ice as a dielectric constant ε equals to 3.1 at this frequency, increasing amount of ice in the soil will also result in a decrease of its bulk dielectric constant.

3. Results and Discussion

[8] A quick comparison of the two hemispheric dielectric maps reveals some fundamental differences (Figure 1). In the south, the area corresponding to the lowest dielectric values defines a quasi-circular aureole from the pole to the 60°S latitude (Figure 1b). This latitudinal variation of MARSIS dielectric value is roughly consistent with the shallow ice limit identified by the Mars Odyssey Gamma-Ray neutron Spectrometer (GRS) [*Mitrofanov et al.*, 2002; *Feldman et al.*, 2002; *Boynton et al.*, 2002], the observed distribution of modern polygonal ground [*Mangold et al.*, 2004; *Levy et al.*, 2009], and the theoretical stability limit of ground ice in equilibrium with present surface temperatures and the water vapour content of the atmosphere [*Schorghofer and Aharonson*, 2005]. Within this range of

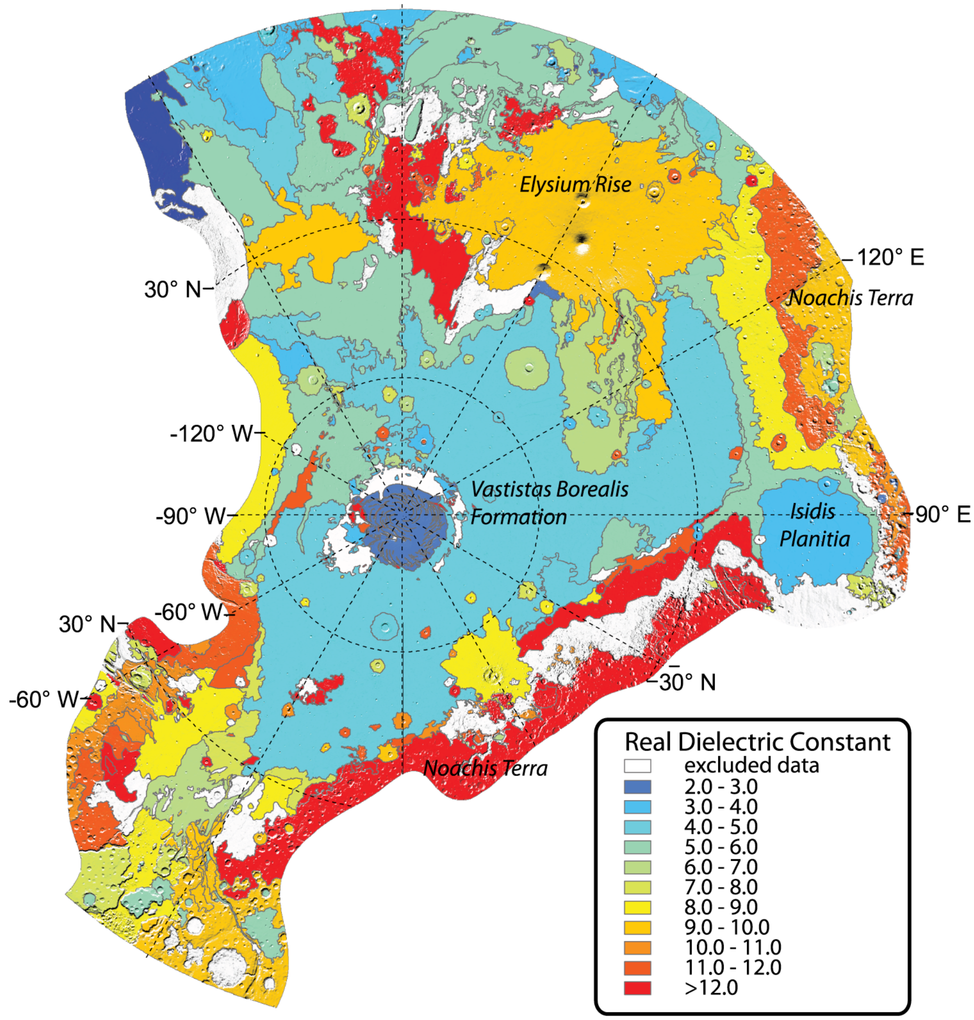

Figure 2. A pole-to-equator map of the Martian northern hemisphere, displayed in polar stereographic projections. The map is color-coded to indicate the MARSIS mean dielectric constant of each geological unit identified by *Tanaka et al.* [2005]. Units where data are biased by rough surface are excluded and represented in white.

latitudes, the data from the MARSIS and GRS instruments are both consistent with the presence of ice-rich permafrost. However, while the GRS instrument is sensitive to the presence of subsurface hydrogen only within the top half-meter, the dielectric values derived from the MARSIS reflectivity data represent the volume averaged properties of the subsurface to a depth of 60–80 m for the range of dielectric properties observed poleward of 60°S (Figure 1b). The total depth of ice-rich permafrost may actually extend much deeper than this, typically 10–20 km [*Clifford et al.*, 2010], depending on the thermal properties of the crust and the inventory of subsurface H_2O.

[9] In the northern hemisphere, the distribution of shallow subsurface ice mapped by gamma-ray and neutron spectroscopy is also roughly consistent with theoretical predictions of ground ice stability (Figure 1b) [*Mitrofanov et al.*, 2002; *Feldman et al.*, 2002; *Boynton et al.*, 2002]. However, the surface dielectric map clearly differs from the distribution of ground-ice observed by GRS (Figure 1). The MARSIS dielectric map displays a pattern of low reflectivity in three similarly sized lobes or branches extending toward lower latitudes in the regions of Amazonis Planitia (150°W), Chryse Planitia (30°W) and Utopia Planitia (100°E). This pattern of low dielectric values is generally consistent with the global topography but displays an even better consistency with the "Deuteronilus" shoreline [*Clifford and Parker*, 2001] (Figure 2), which surrounds the VBF and extends down to encompass the three main catchment areas of the large outflow channels that emanate from the southern highlands. The discharges associated with these outflow channels may have supplemented or covered any surviving frozen remnant of the original Noachian ocean and Hesperian volcanic deposits. It is likely that the episodic fluvial evolution of the northern plains resulted in a complex stratigraphy [*Clifford and Parker*, 2001], consisting of massive ice deposits interbedded with layers of sediment and volcanic materials that may have been emplaced before the underlying ice had sublimed away.

[10] In the southern polar region, the pattern of dielectric constant is dominated by the presence of shallow ground ice at equilibrium with current climate. This shallow ground ice also exists in the Northern hemisphere, as attested by a number of observations including in-situ observations by the Phoenix lander and direct observations by the HiRISE and CRISM instruments inside fresh impact craters. However, because the terrains of the VBF already display low values

Table 1. Summary of the Major Difference Observed by MARSIS in Terms of Dielectric Constant Between Units Expected to be Sedimentary and Volcanic[a]

Unit Symbol	Unit Name	Estimated Dielectric Constant	Interpretation[b]
Abvi	Vastitas Borealis interior unit	4.6 +/−0.5	Sediments of Late Hesperian outflow channels and perhaps other highland and lowland sources highly and pervasively altered during Early Amazonian by periglacial-like processes involving subsurface volatiles
AIi	Isidis Planitia unit	4 +/−0.5	Sedimentary deposit, rapidly emplaced. May result from discharge of ground or from overspill of northern plains ocean across a divide from Utopia basin. Early Amazonian age.
AHEe	Elysium rise unit	9.3 +/−1.0	Lava flows and possibly other volcanic materials. Early Amazonian to Late Hesperian.
Nn	Noachis Terra unit	11.4 +/−1.0	Mixtures of volcanic and sedimentary materials, reworked by impacts. Mainly Late to Middle Noachian.

[a]For each of these units (27), we fit a Gaussian curve to the statistical distribution of dielectric constant. The estimated dielectric constant is taken as the position of the Gaussian maximum and the errors correspond to 1-sigma error estimate of the returned parameter.
[b]*Tanaka et al.* [2005].

of dielectric constant expected of ice-rich regolith, the onset of the shallow ground ice is not detectable on the map.

[11] To further test the apparent spatial correlation between the dielectric map and the geology (i.e. sedimentary vs. volcanic) of the northern plains [*Tanaka et al.*, 2005], we created a composite map (Figure 2) where the average dielectric constant for each geological unit was calculated from the MARSIS data, color-coded, and displayed. Examination of this map reveals that the geological units, which have been identified as sedimentary in nature are associated with low values of dielectric constant ($\varepsilon < 5$). While later Amazonian volcanic units (e.g. Elysium rise) exhibit higher values of ε, Noachian volcanic formations have the very highest values of dielectric constant ($\varepsilon > 9$). These observations confirm the clear link between the dielectric constant and the geological nature of these rocks.

[12] The average dielectric value we measured for the VBF, 4.5+/−1 (see Table 1), provides further insights on the geologic nature of the constituent materials. If the VBF is composed of rock eroded from a source with a dielectric constant of 9 (a value consistent with that of the Tharsis rise basalts, see Table 1), a porosity of about 35% is required according to the classical deLoor mixing formula [*Nunes et al.*, 2011]. To achieve the same observed dielectric constant with a mixture of silicates and water ice, would require a volumetric ice content of ∼60%. Such a mixture could be readily explained if the deposition of sedimentary material was accompanied by the freezing of the ocean, while the sublimation of ice from such mixture could yield a sedimentary lag deposit with a porosity of ∼35%. The inversion of the dielectric constant does not point to a unique composition of the VBF, and may reflect contributions from both cases. Nevertheless, the MARSIS radar data provides the first clear geophysical evidence of an oceanic origin of the VBF.

4. Conclusion

[13] Although much is still unknown about the evolution and environmental context of a Late Hesperian ocean, our observations provide persuasive evidence of its existence by the measurement of a dielectric constant of the VBF that is sufficiently low that it can only be explained by the widespread deposition of (now desiccated) aqueous sediments or sediments mixed with massive ice. This suggests that the water that once filled the Late Hesperian ocean may have suffered two potential fates – either sublimed to the atmosphere (and cold-trapped elsewhere on the planet), or frozen in place and preserved underground. There is significant geologic evidence as dissected terrains, pedestal craters, polygonal soils or scallops [*Mustard et al.*, 2001; *Mangold et al.*, 2004; *Kadish et al.*, 2010; *Lefort et al.*, 2010] that the Martian ground ice is frequently redistributed as a response to the chaotic evolutions of Mars orbital parameters. Ground ice in the first meters to decametres below the surface is susceptible to be affected by these redistributions [*Schorghofer and Aharonson*, 2005]. At greater depth, ice might be stable over geological timescales and a deeply buried cryosphere could account for a large part of the initial water budget of Mars. Rampart craters may be the best evidences of the existence of this ice reservoir [*Costard*, 1989]. Because the depth of the subsurface probed by the radar reflection process could reach 100 m, it is possible that this ice may contribute to the low values of dielectric constant measured by MARSIS.

[14] **Acknowledgments.** Technical and financial support from ESA and CNES is acknowledged. We acknowledge support by grant ANR-10-JCJC-0505-01 from the Agence Nationale de la Recherche (ANR). We thank the anonymous reviewers for the helpful comments.

[15] The Editor thanks Norbert Schorghofer and an anonymous reviewer.

References

Baker, V. R., et al. (1991), Ancient oceans, ice sheets and the hydrologic cycle on Mars, *Nature*, *352*, 589–594.

Boynton, W. V., et al. (2002), Distribution of hydrogen in the near surface of Mars: Evidence for subsurface ice deposits, *Science*, *297*, 81–85.

Carr, M. H. (1987), Water on Mars, *Nature*, *326*, 30–35, doi:10.1038/326030a0.

Carr, M. H. (1996), Channels and valleys on Mars: Cold climate features formed as a result of a thickening cryosphere, *Planet. Space Sci.*, *44*, 1411–1423, doi:10.1016/S0032-0633(96)00053-0.

Carr, M. H., and J. W. Head III (2003), Oceans on Mars: An assessment of the observational evidence and possible fate, *J. Geophys. Res.*, *108*(E5), 5042, doi:10.1029/2002JE001963.

Clifford, S. M., and T. J. Parker (2001), The evolution of the Martian hydrosphere: Implications for the fate of a primordial ocean and the current state of the northern plains, *Icarus*, *154*, 40–79, doi:10.1006/icar.2001.6671.

Clifford, S. M., et al. (2010), Depth of the Martian cryosphere: Revised estimates and implications for the existence and detection of subpermafrost groundwater, *J. Geophys. Res.*, *115*, E07001, doi:10.1029/2009JE003462.

Costard, F. M. (1989), The spatial distribution of volatiles in the Martian hydrolithosphere, *Earth Moon Planets*, *45*(3), 265–290, doi:10.1007/BF00057747.

Di Achille, G., and B. M. Hynek (2010), Ancient ocean on Mars supported by global distribution of deltas and valleys, *Nat. Geosci.*, *3*, 459–463, doi:10.1038/ngeo891.

Feldman, W. C., et al. (2002), Global distribution of neutrons from Mars: Results from Mars Odyssey, *Science*, *297*, 75–78, doi:10.1126/science.1073541.

Head, J. W., III, et al. (1999), Possible ancient oceans on Mars: Evidence from Mars Orbiter Laser Altimeter Data, *Science*, *286*, 2134–2137, doi:10.1126/science.286.5447.2134.

Head, J. W., M. A. Kreslavsky, and S. Pratt (2002), Northern lowlands of Mars: Evidence for widespread volcanic flooding and tectonic deformation in the Hesperian Period, *J. Geophys. Res.*, *107*(E1), 5003, doi:10.1029/2000JE001445.

Kadish, S. J., J. W. Head, and N. G. Barlow (2010), Pedestal crater heights on Mars: A proxy for the thicknesses of past, ice-rich, Amazonian deposits, *Icarus*, *210*, 92–101, doi:10.1016/j.icarus.2010.06.021.

Kreslavsky, M. A., and J. W. Head (2002), Fate of outflow channel effluents in the northern lowlands of Mars: The Vastitas Borealis Formation as a sublimation residue from frozen ponded bodies of water, *J. Geophys. Res.*, *107*(E12), 5121, doi:10.1029/2001JE001831.

Lefort, A., P. S. Russell, and N. Thomas (2010), Scalloped terrains in the Peneus and Amphitrites Paterae region of Mars as observed by HiRISE, *Icarus*, *205*, 259–268, doi:10.1016/j.icarus.2009.06.005.

Levy, J., J. Head, and D. Marchant (2009), Thermal contraction crack polygons on Mars: Classification, distribution, and climate implications from HiRISE observations, *J. Geophys. Res.*, *114*, E01007, doi:10.1029/2008JE003273.

Luo, W., and T. F. Stepinski (2009), Computer-generated global map of valley networks on Mars, *J. Geophys. Res.*, *114*, E11010, doi:10.1029/2009JE003357.

Malin, M. C., and K. S. Edgett (1999), Oceans or seas in the Martian northern lowlands: High resolution imaging tests of proposed coastlines, *Geophys. Res. Lett.*, *26*, 3049–3052, doi:10.1029/1999GL002342.

Mangold, N., et al. (2004), Spatial relationships between patterned ground and ground ice detected by the Neutron Spectrometer on Mars, *J. Geophys. Res.*, *109*, E08001, doi:10.1029/2004JE002235.

Mellon, M. T., et al. (2009), Ground ice at the Phoenix Landing Site: Stability state and origin, *J. Geophys. Res.*, *114*, E00E07, doi:10.1029/2009JE003417, [printed *115*(E1), 2010].

Mitrofanov, I., et al. (2002), Maps of subsurface hydrogen from the high energy neutron detector, Mars Odyssey, *Science*, *297*, 78–81, doi:10.1126/science.1073616.

Mouginot, J., et al. (2010), The 3–5 MHz global reflectivity map of Mars by MARSIS/Mars Express: Implications for the current inventory of subsurface H_2O, *Icarus*, *210*, 612–625, doi:10.1016/j.icarus.2010.07.003.

Mustard, J. F., C. D. Cooper, and M. K. Rifkin (2001), Evidence for recent climate change on Mars from the identification of youthful near-surface ground ice, *Nature*, *412*, 411–414, doi:10.1038/35086515.

Nunes, D. C., et al. (2011), Shallow Radar (SHARAD), pedestal craters, and the lost Martian layers: Initial assessments, *J. Geophys. Res.*, *116*, E04006, doi:10.1029/2010JE003690.

Parker, T. J., R. S. Saunders, and D. M. Schneeberger (1989), Transitional morphology in West Deutronilus Mensae, Mars: Implications for modification of the lowland/upland boundary, *Icarus*, *82*, 111–145, doi:10.1016/0019-1035(89)90027-4.

Parker, T. J., et al. (1993), Coastal geomorphology of the Martian northern plains, *J. Geophys. Res.*, *98*, 11,061–11,078, doi:10.1029/93JE00618.

Perron, J. T., et al. (2007), Evidence for an ancient Martian ocean in the topography of deformed shorelines, *Nature*, *447*, 840–843, doi:10.1038/nature05873.

Picardi, G., et al. (2005), Radar soundings of the subsurface of Mars, *Science*, *310*, 1925–1928, doi:10.1126/science.1122165.

Schorghofer, N., and O. Aharonson (2005), Stability and exchange of subsurface ice on Mars, *J. Geophys. Res.*, *110*, E05003, doi:10.1029/2004JE002350.

Tanaka, K. L., et al. (2001), Huge, CO_2-charged debris-flow deposit and tectonic sagging in the northern plains of Mars, *Geology*, *29*, 430–457, doi:10.1130/0091-7613(2001)029<0427:HCCDFD>2.0.CO;2.

Tanaka, K. L., J. A. Skinner Jr., and T. M. Hare (2005), Geologic map of the northern plains of Mars, *U.S. Geol. Surv. Sci. Invest. Map*, *2888*.

P. Beck and W. Kofman, Laboratoire de Planétologie de Grenoble, Bat. Physique D, 122 rue de la piscine, BP 53, F-38041 Grenoble CEDEX 09, France.

S. M. Clifford, Lunar and Planetary Institute, 3600 Bay Area Blvd., Houston, TX 77058, USA.

J. Mouginot, Department of Earth System Science, University of California, Croul Hall, Irvine, CA 92697-3100, USA.

A. Pommerol, Space Research and Planetary Sciences Division, Physikalisches Institut, Universität Bern, Sidlerstr. 5, CH-3012 Bern, Switzerland.